American Journal of Pathology, Vol. 168, No. 1, January 2006

DOI: 10.2353/ajpath.2006.050398

Cardiovascular, Pulmonary and Renal Pathology

Pathophysiologic Implications of Reduced Podocyte Number in a Rat Model of Progressive Glomerular Injury

Daniela Macconi,* Maria Bonomelli,* Ariela Benigni,* Tiziana Plati,* Fabio Sangalli,* Lorena Longaretti,* Sara Conti,* Hiroshi Kawachi,† Prue Hill,‡ Giuseppe Remuzzi,*§ and Andrea Remuzzi*

From the Mario Negri Institute for Pharmacological Research, Bergamo, Italy; the Department of Cell Biology,† Institute of Nephrology, Niigata University Graduate School of Medical and Dental Sciences, Asahimachi-dori, Niigata, Japan; the Department of Anatomical Pathology,‡ St. Vincent's Hospital, Victoria, Australia; and the Unit of Nephrology and Dialysis,§ Azienda Ospedaliera, Ospedali Riuniti di Bergamo, Bergamo, Italy*

Changes in podocyte number or density have been suggested to play an important role in renal disease progression. Here, we investigated the temporal relationship between glomerular podocyte number and development of proteinuria and glomerulosclerosis in the male Munich Wistar Fromter (MWF) rat. We also assessed whether changes in podocyte number affect podocyte function and focused specifically on the slit diaphragm-associated protein nephrin. Age-matched Wistar rats were used as controls. Estimation of podocyte number per glomerulus was determined by digital morphometry of WT1-positive cells. MWF rats developed moderate hypertension, massive proteinuria, and glomerulosclerosis with age. Glomerular hypertrophy was already observed at 10 weeks of age and progressively increased thereafter. By contrast, mean podocyte number per glomerulus was lower than normal in young animals and further decreased with time. As a consequence, the capillary tuft volume per podocyte was more than threefold increased in older rats. Electron microscopy showed important changes in podocyte structure of MWF rats, with expansion of podocyte bodies surrounding glomerular filtration membrane. Glomerular nephrin expression was markedly altered in MWF rats and inversely correlated with both podocyte loss and proteinuria. Our findings suggest that reduction in podocyte number is an important determinant of podocyte dysfunction and progressive impairment of the glomerular permselectivity that lead to the development of massive proteinuria and ultimately to renal scarring. ***(Am J Pathol 2006, 168:42–54; DOI: 10.2353/ajpath.2006.050398)***

Proteinuric nephropathies progress toward end-stage renal failure independently of the primary insult. Proteinuria is the leakage of plasma proteins into the urine due to dysfunction of the glomerular barrier, which loses its permselective properties. Increasing evidence suggests that the visceral glomerular epithelial cell is a key determinant in the maintenance of the permselective function of the glomerular capillary.[1–5] Podocytes are highly differentiated and specialized epithelial cells anchored to the glomerular basement membrane (GBM). Foot processes of neighboring podocytes interdigitate each other over the capillary wall and are bridged by the slit diaphragm forming the filtration barrier. The most characteristic structural change of damaged podocytes, concomitant with proteinuria, consists of foot process effacement, reorganization of actin cytoskeleton, and apical dislocation of the slit diaphragm.[5–8] We have recently demonstrated that in a genetic model of spontaneous glomerulosclerosis, the male Munich Wistar Fromter (MWF) rat,[9] proteinuria paralleled redistribution of the slit diaphragm protein zonula occludens-1 in the absence of changes in the ultrastructure of the podocyte foot processes as measured by mean foot process width.[10] Along this line, no

Supported in part by the Commission of the European Communities within the EuReGene project (LSHG-CT-2004-005085).

Accepted for publication September 19, 2005.

Part of this work was presented at the 37th Annual Meeting of the American Society of Nephrology, October 27-November 1, 2004, St. Louis, MO.

Address reprint requests to Daniela Macconi, Biol.Sci.D., Mario Negri Institute for Pharmacological Research, Via Gavazzeni, 11, 24125 Bergamo, Italy. E-mail: macconi@marionegri.it.

statistically significant changes in the foot process width have been described in patients with glomerulonephritis and severe proteinuria.[11] Preserved foot processes ultrastructure was also observed in rats made proteinuric by injection with nephritogenic doses of anti-nephrin antibody or with a combination of subnephritogenic doses of anti-neph1 and anti-nephrin antibodies.[12,13] These findings suggest that foot process fusion is not a prerequisite for proteinuria, but they rather indicate that altered expression or dislocation of or perturbed interaction between key components of the slit diaphragm may play a causal role in the development of proteinuria. The mechanism(s) underlying the slit diaphragm reorganization remains a matter for investigation.

There is increasing evidence that reduction in glomerular podocyte number plays an important role in the development of proteinuria and renal disease progression both in animals[14–16] and in humans.[17–22] A positive correlation has been clearly demonstrated between progressive podocyte depletion and the development of glomerulosclerosis in an experimental model of nephrosis in the rat.[14] Among the glomerular structural changes, the podocyte number per glomerulus was the strongest predictor of long-term urinary albumin excretion and rapid progression of the disease in patients with type II diabetes.[18]

The aims of the present study were then to investigate the temporal relationship between glomerular podocyte number and the development of proteinuria and glomerulosclerosis in the MWF rat. We also investigated whether possible changes in podocyte number are associated with alteration in the expression of the slit diaphragm-associated protein nephrin. Functional and structural observations in kidney tissue were compared with those of Wistar rats as controls.

Materials and Methods

Study Design

Thirty-two male Wistar rats (Charles River S.p.A, Calco, Italy) and 38 male MWF rats from our colony[9] were used in this study. Wistar rats were divided in three groups: Group 1 ($n = 14$) was composed of rats of 10 weeks of age; group 2 ($n = 9$), at 20 weeks of age; and group 3 ($n = 9$), at 40 weeks of age. MWF rats were also divided in three additional groups based on the age of the animals: 10 weeks for group 4 ($n = 13$), 20 weeks for group 5 ($n = 13$), and 40 weeks for group 6 ($n = 12$). At the end of the observation period, systolic blood pressure was measured by tail plethysmography in awake animals, and urinary protein excretion was determined by 24-hour urine collections and Coomassie blue G dye-binding assay as described previously.[10] All animals were maintained in a temperature-controlled room regulated with a 12-hour light/dark cycle with free access to water and food (standard rat chow containing 18.5% protein by weight). Animal care and treatment were conducted in conformity with the institutional guidelines that are in compliance with national and international laws and policies (EEC Council Directive 86/609, OJL 358, 1987; DL n116, G.U., Suppl. 40, 18/2/1992; Circolare No.8, G.U., 14/7/1994; Guide for the Care and Use of Laboratory Animals, National Research Council, 1996). At sacrifice, rats were anesthetized and opened through a mid-line incision. Abdominal aorta was cannulated below renal arteries with a catheter connected to a pressure transducer (Battaglia Rangoni, Bologna, Italy). Both kidneys were perfused with phosphate-buffered saline (PBS) at the measured arterial pressure for 3 minutes. Then, the right kidney was removed. Midcoronal sections were fixed by immersion with paraformaldehyde-lysine-periodate (PLP; 2% paraformaldehyde, 0.075 mol/L lysine, and 0.01 mol/L sodium periodate in 0.0375 mol/L sodium phosphate buffer) overnight at 4°C and processed for immunohistochemistry as detailed below. Cortex was isolated from the remaining tissue and snap-frozen in liquid nitrogen for real-time polymerase chain reaction (PCR) analysis of nephrin and WT1 expression. The left kidney was fixed by perfusion with 1.25% glutaraldehyde in 0.1 mol/L cacodylate buffer and removed. Midcoronal sections were postfixed in Dubosq-Brazil fluid or 2.5% glutaraldehyde for morphological analysis by light microscopy or scanning electron microscopy (SEM), respectively. Small pieces of kidney were postfixed in 2.5% glutaraldehyde before processing for transmission electron microscopy (TEM).

Four to seven rats per group were used at sacrifice to isolate glomeruli for Western blot analysis of nephrin expression. To this end, both kidneys were perfused under controlled pressure with ice-cold PBS supplemented with protease inhibitors. A small section was fixed in PLP for immunohistochemistry of nephrin and WT1. Cortex was isolated from the remaining tissue for glomeruli isolation.

Morphometric Analysis of Glomerulosclerosis

Sections (3.5 μm) were stained with periodic acid-Schiff (PAS) technique as described previously.[9] The presence of sclerosis in glomerular tuft area was investigated, and if present, its extension was determined using computer-based morphometric analysis. Tissue sections were examined on a Zeiss light microscope (Zeiss, Jena, Germany) connected to a video camera and a computer-based image analysis system. For each kidney section, 50 glomeruli were systematically digitized (glomeruli were consecutively encountered by moving the microscope stage with an S-shape path) using a 40× objective and examined. For glomerular capillary sections affected by sclerosis, the fraction of tuft volume affected by sclerosis was estimated by point counting using a 19 × 19 line orthogonal grid digitally overlaid on the glomerular section image (Scion Image v. 1.62). For each glomerular section, the number of grid points hitting the capillary tuft and those hitting the sclerotic region were counted. Fraction of glomerular tuft area affected by sclerosis was expressed as the percent ratio between grid points in the sclerotic area over total points in the glomerular tuft.

Electron Microscopy (EM)

Glutaraldehyde-fixed fragments of cortical kidney tissue from four Wistar and four MWF rats at 20 weeks were washed repeatedly in cacodylate buffer and postfixed in 1% OsO_4 for 1 hour. Then specimens were dehydrated through ascending grades of alcohol and embedded in Epon resin. Ultrathin sections were stained with uranyl acetate for examination using a Philips Morgagni transmission electron microscope. To evaluate the density of peripheral capillary membrane covered by podocyte body and in direct contact with the Bowman's space, we used digital images of semithin sections (obtained by photo-montage with final resolution of 4500 × 3000 pixels) overlaid with a bundle of straight lines intersecting in the center of the capillary tuft. Line orientation was uniformly distributed with a constant angle between two lines of 5°. The area of the vascular pole was not considered. The intersection between each line and peripheral capillary membrane was analyzed to establish whether capillary membrane was in direct contact with outer urinary space or covered by the podocyte body. For SEM, kidney samples were processed as for TEM until the step of dehydration in alcohol, and then samples were dried under vacuum and coated with atomic gold particles as previously described.[23]

Immunohistochemistry of Nephrin and Wilms' Tumor 1 (WT-1)-Positive Cells

Sections (3 μm) from PLP-fixed kidney specimens were immunostained for nephrin by indirect immunofluorescence with monoclonal antibody 5-1-6[24] (0.1 mg/ml, overnight at 4°C), followed by incubation with Cy3-conjugated $F(ab')_2$ fragment donkey anti-mouse IgG (affinity purified 6.5 μg/ml in PBS; Jackson ImmunoResearch Laboratories, West Grove, PA) for 1 hour at room temperature. Fluorescence was analyzed by an inverted light microscope (IX70; Olympus Optical, Tokyo, Japan) equipped with epifluorescence and a computer-based image analysis system. The extent of glomerular expression of nephrin was evaluated by a blind observer. Scores were assigned to individual glomeruli of each section as follows: 1, signal covering 0 to 25% of the glomerular tuft area; 2, 25 to 50%; 3, 50 to 75%; and 4, 75 to 100%. The final score per section was then calculated as the weighted mean

$$S_{\text{nephrin}} = \frac{[(1 \times N_1) + (2 \times N_2) + (3 \times N_3) + (4 \times N_4)]}{N_{1+}N_{2+}N_{3+}N_4}$$

where N_i (i = 1 to 4) is the number of glomeruli in each category. From 50 to 150 glomeruli in one or two sections were randomly chosen and examined. Care was taken not to resample the same glomeruli by moving the microscope stage with an S-shape path. Negative controls, with the secondary antibody alone, resulted in a complete prevention of staining at the glomerular level.

To assess whether changes in nephrin staining were associated with area of glomerulosclerosis, we compared nephrin expression and glomerulosclerosis in the same glomerular tuft. To this purpose, we obtained two serial sections from PLP-fixed kidney tissue of three MWF rats at 40 weeks. The first section was immunostained for nephrin, and the second section was stained with PAS. Images of 36 glomeruli randomly selected on nephrin-immunostained sections were digitally acquired. For each glomerular tuft imaged, the corresponding glomerular section at optical microscopy using PAS-stained sections was identified and digitized at the same final magnification. To quantify the area density occupied by different nephrin staining and sclerosis, we overlaid each glomerular section with an orthogonal grid made of 20 × 20 equispaced lines. On immunostained images, the number of grid points hitting normal nephrin staining, fragmented, or absent were counted, and the area density of each glomerular section was calculated as percentage. The same grid was overlaid on the corresponding PAS image, and the density of points hitting sclerotic area or normal capillary tuft was calculated.

Glomerular podocytes were identified as WT1-positive cells as follows. After antigen unmasking and blocking of nonspecific sites, sections were incubated with rabbit polyclonal antibody to WT1 (C-19) directed against the C terminus of WT1, a podocyte-specific marker[25] (2 μg/ml in PBS; Santa Cruz Biotechnology, Santa Cruz, CA), for 1 hour (room temperature), followed by Cy3-conjugated goat anti-rabbit IgG (15 μg/ml in PBS; Jackson Immunoresearch Laboratories Inc.). After washing, sections were incubated with fluorescein-conjugated wheat germ agglutinin (WGA; 12.5 μg/ml in PBS; Vector Laboratories Inc., Burlingame, CA) for 15 minutes at room temperature, then washed, and finally incubated with 4′,6-diamidine-2′-phenylindole dihydrochloride (DAPI; Boehringer, Mannheim, Germany) for 30 minutes at 37°C. Using fluorescence microscopy with appropriate filters, images of single wavelength were acquired and digitally merged. In the merged image, podocytes were then identified and counted. At least 15 glomerular sections were examined in a blinded manner for each animal. In additional experiments, we performed triple labeling for WT1, vimentin (monoclonal mouse anti-vimentin clone V9; 1:300; Dako S.p.A, Milan, Italy), and DAPI in kidney sections from MWF rats (n = 2 for each age) and 20-week-old Wistar rats (n = 2) selected for having a podocyte number per glomerulus close to the group average. Sections were analyzed by an observer unaware of the identity of samples using a confocal laser scanning microscopy (LS 510 Meta; Zeiss). Five to nine glomeruli for each MWF group and three for Wistar rats were randomly examined. For each glomerulus, separate images for each marker were acquired and digitally merged. Then, by comparing superimposed images of WT1 and DAPI with those of vimentin plus DAPI, we counted the number of cells positive for WT1, vimentin, or both.

Estimation of Glomerular Volume and Number of Podocyte/Glomerulus

Estimation of glomerular volume (V_G) was performed using a computer-based image analysis system (Mac OS

09; Apple Computer, Cupertino CA). Histological sections of fluorescein-WGA-labeled glomeruli were digitized from the fluorescence microscope and stored on 696 × 520-pixel images. Exact enlargement in micrometers per pixel of digital images was calculated from images of a reference grid digitized at the same resolution. The outline of the minimal polygon around the glomerular tuft area was manually traced, and its surface area automatically measured, in the same glomeruli examined for counting WT1-positive cells in each tissue section. Mean value of V_G was then calculated using the formula[26]

$$V_G = (\beta/k)(A_m)^{3/2}$$

where $k = 1.1$ (size distribution coefficient) and $\beta = 1.38$ (shape coefficient for spheres), which is the assumed shape of glomeruli.[9]

The estimation of the average number of podocytes per glomerulus (N_P) was determined by the stereological method of particle density proposed by Weibel.[26] Briefly, the volume density of the podocytes (N_V) in glomerular tuft volume was estimated as $N_V = N_A/\bar{D}$ where podocyte nuclear profile area density (N_A) was estimated by the ratio between the numbers of podocyte nuclear profiles and the glomerular profile area in each glomerulus. $\bar{D}$ is the average diameter of podocyte nuclei that we estimated from major and minor axes of cell nuclear sections. To calculate $\bar{D}$, the average volume of podocyte nuclei ($\bar{V}$) was first calculated based on the assumption that podocyte nuclei have an ellipsoidal shape. The average diameter of an equivalent sphere having the same volume of the ellipsoid was then determined. The mean number of podocytes per glomerular tuft (N_P) was calculated for each animal by multiplying podocyte volume density N_V in the capillary tuft by the mean value of V_G previously calculated.

Isolation of Glomeruli and Western Blot Analysis

Glomeruli were isolated from kidney cortices by graded sieving as previously described,[10] and the purity of preparation accounted for >90% decapsulated glomeruli. Briefly, glomerular pellets were incubated in RIPA buffer (0.1% sodium dodecyl sulfate, 0.5% deoxycholate, 1% Triton X-100, 20 mmol/L HEPES [pH 7.5], and 150 mmol/L NaCl) in the presence of protease inhibitor cocktail (Sigma-Aldrich) and 1 mmol/L EDTA for 30 minutes. Samples were lysed on ice by sonication and centrifuged (15,000 × *g* for 15 minutes at 4°C) to remove detergent-insoluble materials. Protein concentration was determined by BCA assay (Pierce Chemical Co., Rockford, IL). Equal amounts of proteins were separated on 5% sodium dodecyl sulfate-polyacrylamide gel electrophoresis under reducing conditions and transferred to polyvinylidene difluoride membranes (Bio-Rad Laboratories, Hercules, CA). Membranes were incubated overnight at 4°C with rabbit anti-rat nephrin antibody raised against an intracellular site peptide of 21 amino acids[27] (1:2000), followed by horseradish peroxidase-conjugated goat anti-rabbit IgG (room temperature, 1 hour). Bound antibodies were detected by enhanced chemiluminescence (SuperSignal, Pierce Chemical Co.). Bands were quantified by densitometric analysis with Microscan 1.0.5 and NIH Image (v. 1.61) software.

Quantitative Real-Time PCR

Total RNA was extracted from the cortical portion of the kidney by the guanidium isothiocyanate/cesium chloride procedure. Contaminating genomic DNA was removed by incubating with RNase-free DNase (Promega, Ingelheim, Germany) for 1 hour at 37°C. The purified RNA (1 μg) was reverse-transcribed using random hexamer oligonucleotides and 200 U of Super-Script II RT (Invitrogen, San Giuliano Milanese, Italy) for 1 hour at 42°C. No enzyme was added for reverse transcriptase-negative controls (RT^-).

Real-time PCR was performed on TaqMan ABI 5700 Sequence Detection System (PE Biosystems, Warrington, UK) using heat-activated *Taq*DNA polymerase (Amplitaq Gold; PE Biosystems). The SYBR Green Master mix was used according to the manufacturer's protocol. After an initial hold of 2 minutes at 50°C and 10 minutes at 95°C, the samples were cycled 40 times at 95°C for 15 seconds and 60°C for 60 seconds to reach the plateau. Fluorescence detection, defined as threshold cycle (Ct), is automatically selected in the exponential phase of PCR and used for the relative quantification of the target gene. The comparative Ct method normalizes the number of target gene copies to a housekeeping gene as glyceraldehyde-3-phosphate dehydrogenase (ΔCt). Gene expression was then evaluated by the quantification of cDNA corresponding to the target gene relative to a reference sample (10-week-old Wistar or MWF rats, ΔΔCt for WT1 and 10-week-old Wistar rats for nephrin). On the basis of exponential amplification of target gene, $2^{-\Delta\Delta Ct}$ gives the amount of amplified molecules at the Ct. The following oligonucleotide primers (300 nmol/L) were used. For rat WT1: sense, 5′-TCCGCAACCAAGGATACAGC-3′, and antisense, 5′-CATAACTGGGTGCCCCGTC; for rat nephrin: sense, 5′-GGAGGACAGGATCAGGAATGAA-3′, and antisense, 5′-CCCGGTCCCCAGTCCA-3′; and for glyceraldehyde-3-phosphate dehydrogenase: sense, 5′-TCATCCCTGCATCCACTGGT, and antisense, 5′-CTGG-GATGACCTTGCCCAC. All primers were obtained from Sigma Genosys (Cambridgeshire, UK). True identity of the amplification products was ensured by primer specificity for WT1 and nephrin rat sequences, the presence of a single dissociation curve at a constant $T_{melting}$, and the lack of genomic DNA contamination or primer dimer in RT^- samples.

Statistical Analysis

Results are expressed as means ± SD. Values within the same strain of rats were compared by analysis of variance and Bonferroni test. Comparison between age-matched Wistar and MWF rats was performed by unpaired Student's *t*-test. Values of nephrin staining in individual glomeruli were compared by Kruskal-Wallis or Mann-Whitney test as appropriate for nonparametric data. Regression analysis was

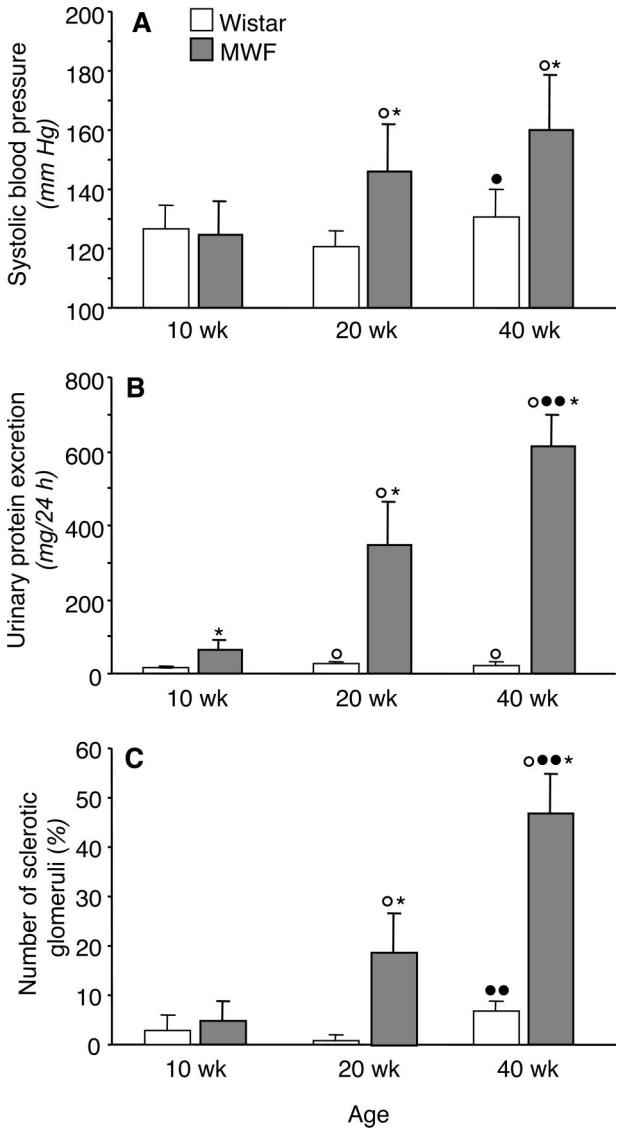

Figure 1. Systolic blood pressure (**A**), proteinuria (**B**), and incidence of glomerulosclerosis (**C**) in Wistar and MWF rats. Results are means ± SD. *$P <$ 0.01 versus Wistar rats of the same age; ○, $P < 0.01$ versus the 10-week-old rats within the same strain; ●, $P < 0.05$ and ●●, $P < 0.01$ versus the 20-week-old rats within the same strain.

performed using the simple linear regression test. Statistical significance was defined as $P < 0.05$.

Results

Blood Pressure and Proteinuria

As reported in Figure 1A, systolic blood pressure was comparable in MWF and Wistar rats at 10 weeks of age. Moderate hypertension developed in MWF rats at 20 and 40 weeks of age, compared with age-matched Wistar rats. In MWF rats, urinary protein excretion was already higher than normal at 10 weeks, compared with Wistar rats of corresponding age. Massive proteinuria developed spontaneously with age, averaging 356 ± 113 and 615 ± 85 mg/day in animals at 20 and 40 weeks of age, respectively (Figure 1B).

Morphological and Morphometric Analysis of Glomerular Structure

Structural changes of the glomerular tuft were first investigated by morphometric analysis to estimate the incidence and the extent of glomerulosclerosis. Data are reported in Figure 1C. In young animals 10 weeks of age, the percentage of glomeruli affected by sclerosis was modest and comparable between control and MWF rats. Then the incidence of glomerulosclerosis significantly increased with age in MWF rats, affecting 19 ± 8 and 47 ± 8% of glomeruli on average in 20- and 40-week animals, respectively. Evaluation of glomerular volume occupied by sclerosis in individual glomeruli showed that at 20 weeks, the majority of sclerotic glomeruli (89%) had structural changes occupying less than 25% of the tuft area, whereas the remaining ones were affected by sclerotic changes occupying between 25 and 50% of the tuft area. At 40 weeks, the percentage of glomeruli affected by mild sclerosis—occupying <25% of tuft area—was reduced to 62%, and severe changes were found in 4% of sclerotic glomeruli.

The results of glomerular volume estimation and podocyte densities are reported in Figure 2. Mean V_G significantly increased in Wistar rats from 10 to 20 weeks of age, averaging 0.73 ± 0.17 and 1.16 ± 0.23 × 10^6 μm^3, respectively, but they did not change significantly thereafter (Figure 2A). In MWF rats, glomerular volume progressively increased with age, with a remarkable volume increase at 40 weeks. Values of V_G in MWF rats were significantly higher than those calculated for the control group at same age (Figure 2A).

To estimate the podocyte number per glomerulus, we first counted the number of cells positive for WT1. As shown in Figure 3, A–D, WT1 was specifically localized in nuclei of podocytes, appearing red, fluorescein-WGA stained the glomerular tuft green, and DAPI stained all cell nuclei blue. In the merged image, podocytes are clearly identified as cells having a nucleus stained in dark pink (Figure 3D). To validate this method for podocyte counting, we verified whether all glomerular cell nuclei in contact with cytoplasm expressing vimentin were also positive for WT1 staining. Figure 3, E and F, shows a detail of representative images of the same glomerular section from a Wistar rat immunostained for both vimentin and WT1. All vimentin-positive cells were also positive for WT1 in MWF and Wistar rats. Relative WT1 mRNA levels in cortical tissue from Wistar rats at 20 and 40 weeks of age were numerically but not significantly higher than those expressed in 10-week-old animals of the same strain ($2^{-\Delta\Delta Ct}$: 1.51 ± 0.29 and 1.63 ± 0.69 at 20 and 40 weeks, respectively). WT1 mRNA expression did not change with age in MWF rats ($2^{-\Delta\Delta Ct}$: 1.05 ± 0.15 and 1.04 ± 0.17 at 20 and 40 weeks, respectively).

Wistar rats at 10 weeks of age had 203 ± 36 podocytes per glomerulus, and this number did not change

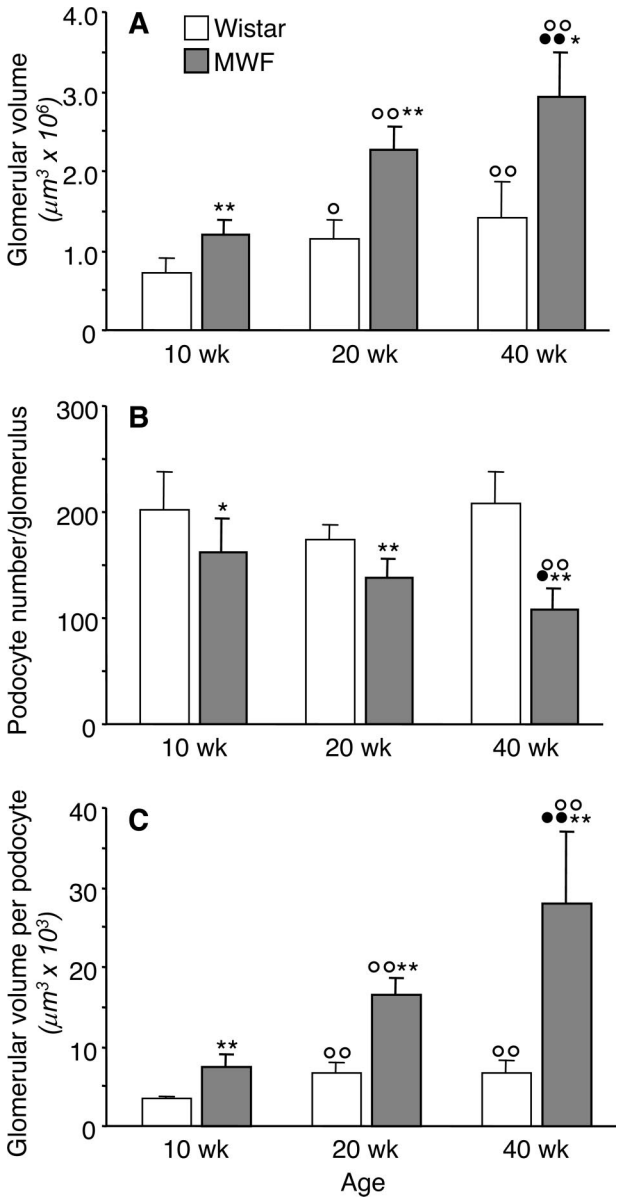

Figure 2. Glomerular tuft volume (V_G) (**A**), podocyte number per glomerulus (**B**), and podocyte density, V_G/podocyte (**C**) in Wistar and MWF rats. Results are means ± SD (n = 7 to 9 rats for Wistar groups and n = 9 to 10 rats for MWF groups). *$P < 0.05$ and **$P < 0.01$ versus Wistar rats of the same age; ○, $P < 0.05$ and ○○, $P < 0.01$ versus the 10-week-old rats within the same strain; ●, $P < 0.05$ and ●●, $P < 0.01$ versus the 20-week-old rats within the same strain.

significantly with age (Figure 2B). At variance, in MWF rats at 10 weeks, mean podocyte number per glomerulus averaged 162 ± 32, a value significantly lower than control rats at the same age. Podocyte number further decreased with age in MWF rats. As shown in Figure 2C, the increase in calculated glomerular volume per podocyte was remarkable along the study period in MWF animals, reaching more than a threefold increase over Wistar rats at 40 weeks. Linear regression analysis showed that the glomerular volume related to each podocyte in MWF rats strongly and significantly correlated with both proteinuria ($r = 0.78$, $P < 0.01$) and the incidence of glomerulosclerosis ($r = 0.83$, $P < 0.01$) (Figure 4).

TEM and SEM

At EM, podocytes of MWF rats at 20 weeks were structurally different from those of control Wistar animals. SEM showed that the podocyte body in MWF rats covered most of the external capillary tuft surface, leaving less peripheral capillary membrane in direct contact with the urinary space (Figure 5, A and B). This observation was confirmed by the morphometrical analysis performed on semithin sections. We actually observed that 53 ± 12% (n = 12) of the peripheral tuft was not covered by podocyte body in Wistar rats, whereas this percentage was significantly lower ($P < 0.01$) in MWF rats of the same age, averaging 37 ± 14%. Similar changes were seen by TEM in Figure 5, C and D, in which the peripheral capillary loops of glomeruli from Wistar and MWF strain are representative of the glomerular population analyzed. In glomeruli from Wistar animal capillary loops, foot process/filtration slits appeared almost entirely in direct contact with urinary space, whereas in MWF rats, podocyte bodies were swollen and expanded, frequently extending around peripheral capillary loops.

Nephrin Protein and mRNA Expression

In Wistar animals, nephrin expression consisted of a linear pattern of distribution along the peripheral capillary loop (as shown in Figure 6A), with uniform fluorescence signal along the capillary membrane in the entire tuft section; nephrin expression pattern did not change in older animals (data not shown). On the contrary, in MWF rats, nephrin staining was already altered in young animals and further changed with age. As shown in Figure 6, B–D, protein staining was heterogeneous within glomeruli of the same animal, with pattern changing from linear to fragmented or punctated in focal areas of the glomerulus. This pattern worsened with age. In older MWF rats, partial or almost complete loss of the protein was observed. The results of semiquantitative evaluation of nephrin expression at single glomerular level are reported in Figure 6, E–H. In Wistar rats of 10 weeks of age, 98 ± 3% of glomeruli showed normal staining for the entire tuft (fourth rank) (Figure 6E). Similar results were obtained in older animals: glomeruli with immunofluorescent signal covering more than 75% of the glomerular tuft accounted for 94 ± 4 and 92 ± 8% in 20- and 40-week-old rats, respectively. By contrast, in MWF rats, the percentage of glomeruli grouped in the fourth rank decreased with age from 81 ± 11% at 10 weeks to 60 ± 15 and 39 ± 18% at 20 and 40 weeks, respectively (Figure 6, F–H). The progressive worsening of nephrin staining was further documented by the concomitant presence of glomeruli grouped in lower ranks (Figure 6, F–H).

The comparison of nephrin changes and extension of sclerosis within the same glomerular tuft allowed us to document that where nephrin staining was absent the area was always coincident with a sclerotic area slightly

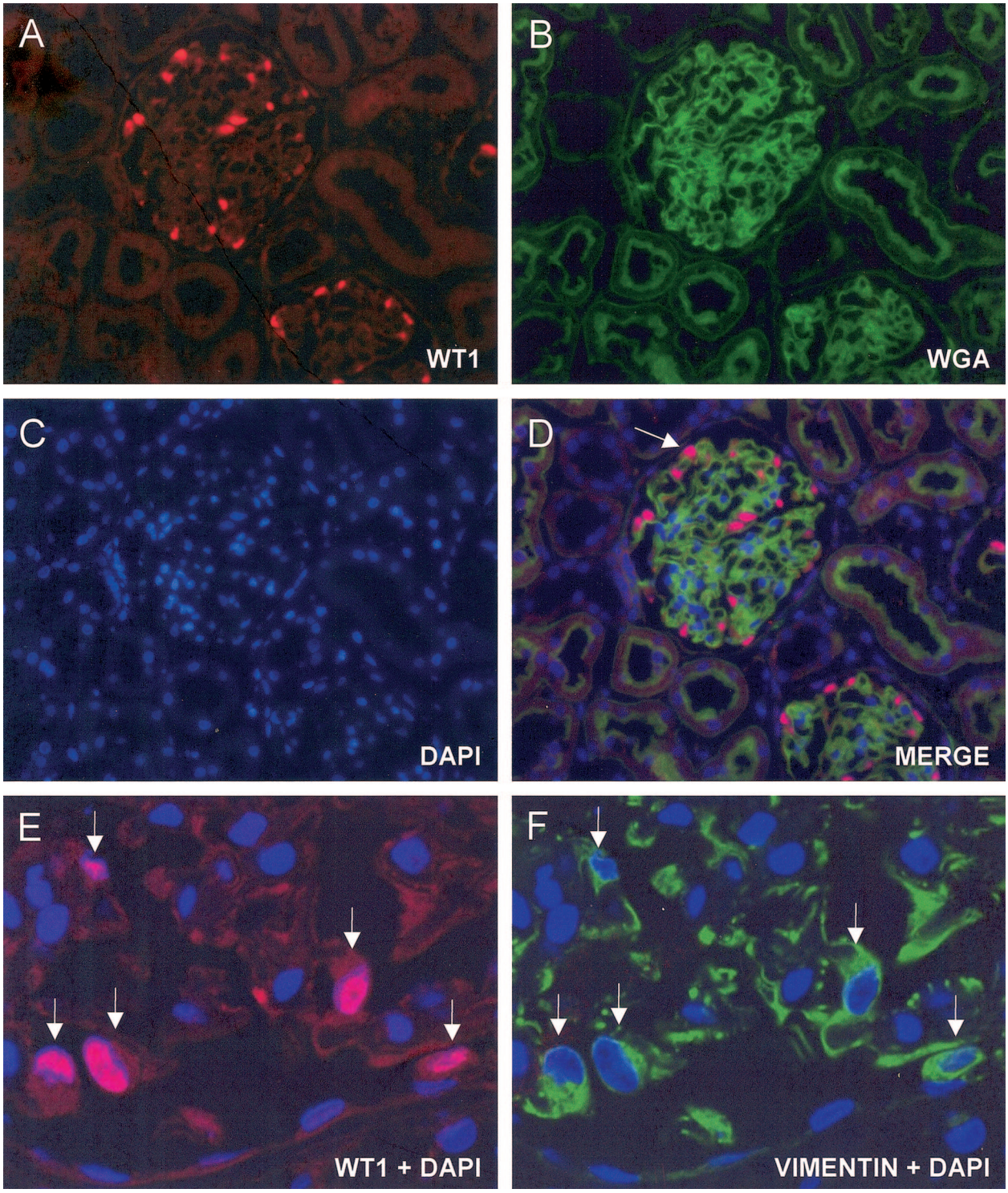

Figure 3. Immunohistochemistry of podocytes. Representative micrographs of a 3-μm section from PLP-fixed Wistar kidney showing triple labeling of a glomerulus for podocytes (WT1-positive nuclei in red; **A**), for glomerular capillaries (fluorescein-WGA staining; **B**) and for cell nuclei (DAPI in blue; **C**). **D:** In the merged image, podocytes are clearly detected as cells having a dark pink nucleus (**arrow**). Details of podocytes in a glomerular section from a Wistar rat stained for WT1, vimentin, and DAPI. Superimposed images of WT1 and DAPI show pink staining of podocyte nuclei (**E**, **arrows**). **F:** The same cells are vimentin-positive, as documented by the green fluorescence surrounding the nucleus. Final magnification, ×200 (**A–D**) and ×630 (**E** and **F**).

smaller (Figure 7). Moreover, there were areas of capillary tuft stained by nephrin in a fragmented pattern that were not associated with sclerotic changes by light microscopy. In details, in an average 24% of tuft area, nephrin was absent; in 25%, nephrin appeared fragmented; and in the remaining 51%, nephrin expression was normal. In the same glomeruli, 19% of tuft area was occupied by sclerosis, and fragmented nephrin was lo-

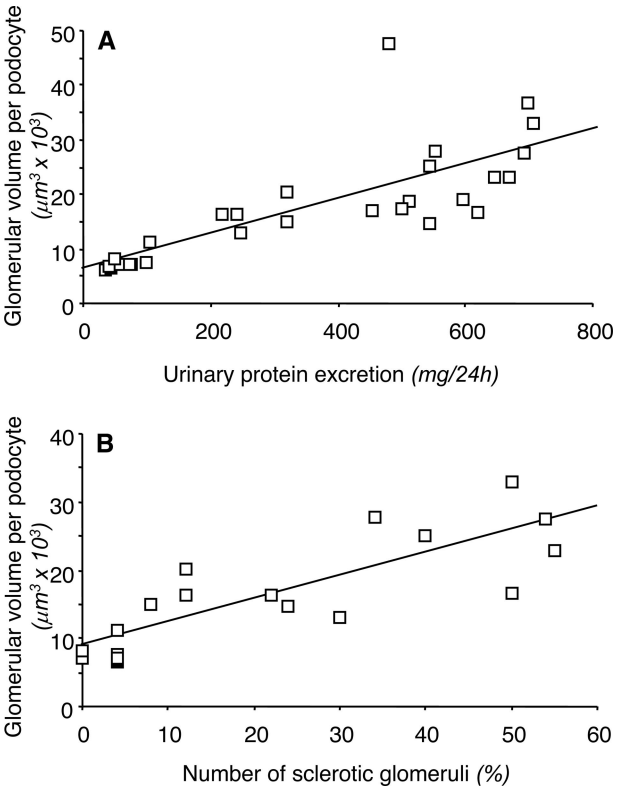

Figure 4. Plot of glomerular volume per podocyte (*y* axis) against urinary protein excretion (*x* axis) (**A**) and the percentage of sclerotic glomeruli (*x* axis) (**B**) in MWF rats. In both cases, a significant positive correlation was found.

cated in capillary tuft areas not yet sclerotic (Figure 7B). As shown in Figure 8, B and C, linear regression analysis showed a positive correlation between glomerular nephrin expression and mean podocyte number per glomerulus ($r = 0.59$, $P < 0.01$) (Figure 8A). Both parameters inversely correlated with urinary protein excretion ($r = -0.80$ and $r = -0.69$, for nephrin and podocyte number, respectively; $P < 0.01$).

To investigate whether changes in nephrin staining reflected changes in the amount of protein expressed in glomeruli of MWF rats, we further analyzed nephrin expression by Western blot. As shown in Figure 9A, nephrin from glomerular lysates of Wistar rats migrated as a doublet consisting of a major band of about 180 kd and a weak immunoband of lower molecular mass.[27] Nephrin expression significantly increased in Wistar rats from 10 to 20 weeks of age and did not change thereafter. No significant difference was found in nephrin expression in MWF rats from 10 to 20 weeks of age; however, the protein significantly decreased in older animals. The density of nephrin bands was significantly lower in 20- and 40-week MWF rats in comparison with Wistar rats of the same age (Figure 9B).

Changes in nephrin mRNA expression paralleled those in nephrin protein expression (Figure 9C). Relative nephrin mRNA levels increased with age in Wistar rats, although the difference did not reach statistical significance. In MWF rats, nephrin mRNA slightly increased at 20 weeks, but by 40 weeks, values returned to levels fully comparable with those measured in 10-week-old animals. At this age, nephrin mRNA expression was significantly lower than in Wistar rats.

Discussion

The present study shows that in the male MWF rat, a progressive reduction in the number of podocytes per glomerulus correlated with proteinuria and preceded the development of glomerulosclerosis. Decrease in the podocyte number with time was paralleled by the progressive loss of the expression of slit diaphragm protein nephrin.

Glomerular volume increased both in MWF and Wistar rats although at a different rate. Confirming our previous observation,[28] glomerular hypertrophy had already developed by 10 weeks in MWF animals. Such early adaptive changes serve to achieve a higher single nephron glomerular flow and filtration necessary to compensate the inborn nephron deficit.[28] Glomerular volume progressively increased from 10 to 20 weeks of age in MWF rats as a consequence of animal growth,[29] with a similar trend observed in Wistar rats of comparable age. However the subsequent significant increase in glomerular volume, which was only confined to the MWF rat, reflects a further increase both in the number and in the volume of glomerular cells, as we have previously reported for mesangial cells.[9] The recent observation that alterations in podocytes may contribute to glomerular volume hypertrophy in subtotally nephrectomized rats[15,30] prompted us to evaluate podocyte behavior in MWF rats.

Here, we estimated the number of podocytes per glomerulus by counting WT-1-positive cells. WT-1 is involved in nephrogenesis, is widely expressed in glomerular progenitor cells, and is restricted to the nuclei of differentiated podocytes as the glomerulus matures.[25] Our results showed that in MWF rats, the podocyte number per glomerulus was already lower than normal at a young age and progressively decreased with time. In some disease conditions, as in HIV nephropathy and in collapsing focal segmental glomerulosclerosis,[31] podocyte nuclei are WT-1-negative as cells undergo phenotypic dysregulation. Therefore, we wondered whether the reduction of WT-1-positive cells, which we observed in the MWF rats, represents a real loss of podocytes rather than podocytes that have undergone phenotypic changes. To examine this, we concomitantly evaluated both WT-1 and vimentin, a cytoskeletal intermediate filament protein highly expressed in podocytes and not modulated in various experimental models of glomerular epithelial cell injury.[32] Double staining with vimentin and WT-1 showed that in MWF rats, all vimentin-positive cells also expressed WT1. These data, together with the evidence that WT-1 mRNA did not vary with age, would definitely indicate an effective, progressive loss of podocytes in MWF rats. Of note, the lower podocyte number in this strain at 10 weeks could be attributed to the impaired nephrogenesis that is due to the genetic defect, resulting in reduced nephron number (about 50% in average) and in superficial capillary tufts not covered by the peripheral

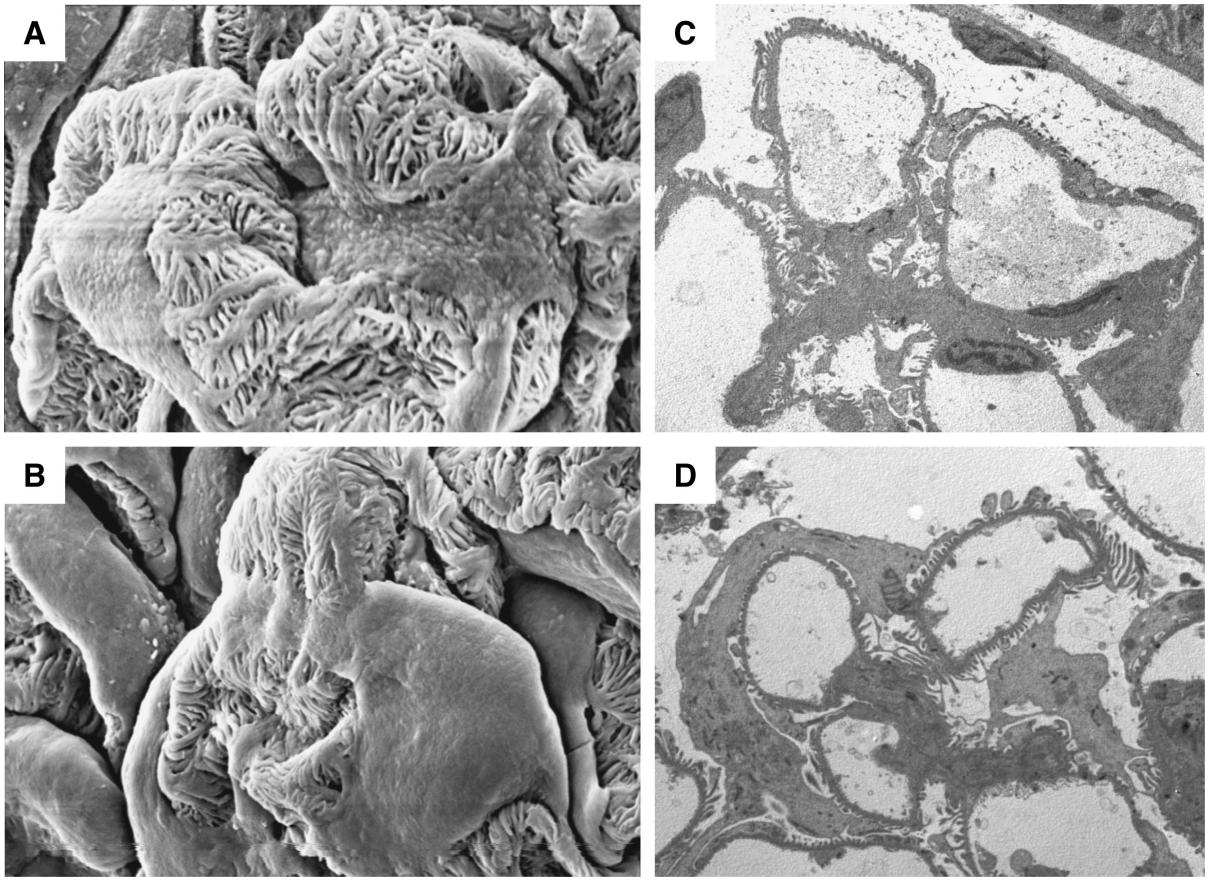

Figure 5. Representative SEM (**A** and **B**; final magnification, ×3000) and TEM (**C** and **D**; final magnification, ×2200) micrographs of podocyte ultrastructure in Wistar (**A** and **C**) and MWF rats (**B** and **D**) of 20 weeks of age. Podocyte body covers most of the peripheral capillary wall surface in MWF animals (**B** and **D**).

layer of proximal tubules (as in normal animals) that is formed during the last phase of nephrogenesis.[28,33]

Podocyte loss has been found to be a common feature in both experimental and human progressive renal diseases[14–22] and may occur as a consequence of both apoptosis[34,35] and podocyte detachment from the GBM.[7,36] In the latter case, podocytes may be found in the urine.[37–39] Here, we observed a positive correlation in MWF rats between the capillary tuft volume per podocyte and both urinary protein excretion and incidence of glomerulosclerosis. The intercepts of these plots were 6.1 or 8.6×10^3 μm^3, respectively, and might represent the threshold values of glomerular volume, above which proteinuria or glomerulosclerosis would be expected to occur. MWF rats at 10 weeks of age with a glomerular volume per podocyte of 7.5×10^3 μm^3 had urinary protein excretion above normal but had renal morphological changes comparable with Wistar rats. Older MWF rats with a glomerular volume per podocyte value of 28×10^3 μm^3 had massive proteinuria. In these animals, a consistent fraction of the glomerular population was affected by sclerosis, and this might contribute in part to podocyte loss.

In the MWF rat, the increase in glomerular tuft volume and progressive reduction in number of podocytes result in adaptive changes of the podocyte structure that may influence permeability function of the glomerular capillary membrane.[40,41] Our present observation of podocyte ultrastructure at EM shows that in MWF rats, podocyte body extends around glomerular capillary segment and peripheral glomerular membrane. These morphological observations were confirmed by morphometrical analysis showing a reduction in the peripheral capillary membrane directly in contact with the urinary space while the remaining peripheral membrane is covered by podocyte body. If the area of GBM that must be covered by single podocytes increases, podocyte architecture must change. The mechanism(s) through which these alterations relate to proteinuria in these animals has to be established.

In the MWF rats, the expression of nephrin was markedly altered. We have specifically investigated whether areas of capillary tuft not expressing nephrin were actually occupied by sclerosis. Direct comparisons of adjacent glomerular sections with nephrin immunostaining and PAS showed that this was the case. However, we also observed that in MWF rats, areas of glomerular tuft that appear normal at light microscopy are characterized by fragmentation of nephrin staining along the capillary wall. This would suggest that structural changes of podocytes are also characterized by alteration of nephrin expression before sclerosis develops. Analysis of protein content by Western blot in glomerular lysate showed that reduction of nephrin protein was only observed in ani-

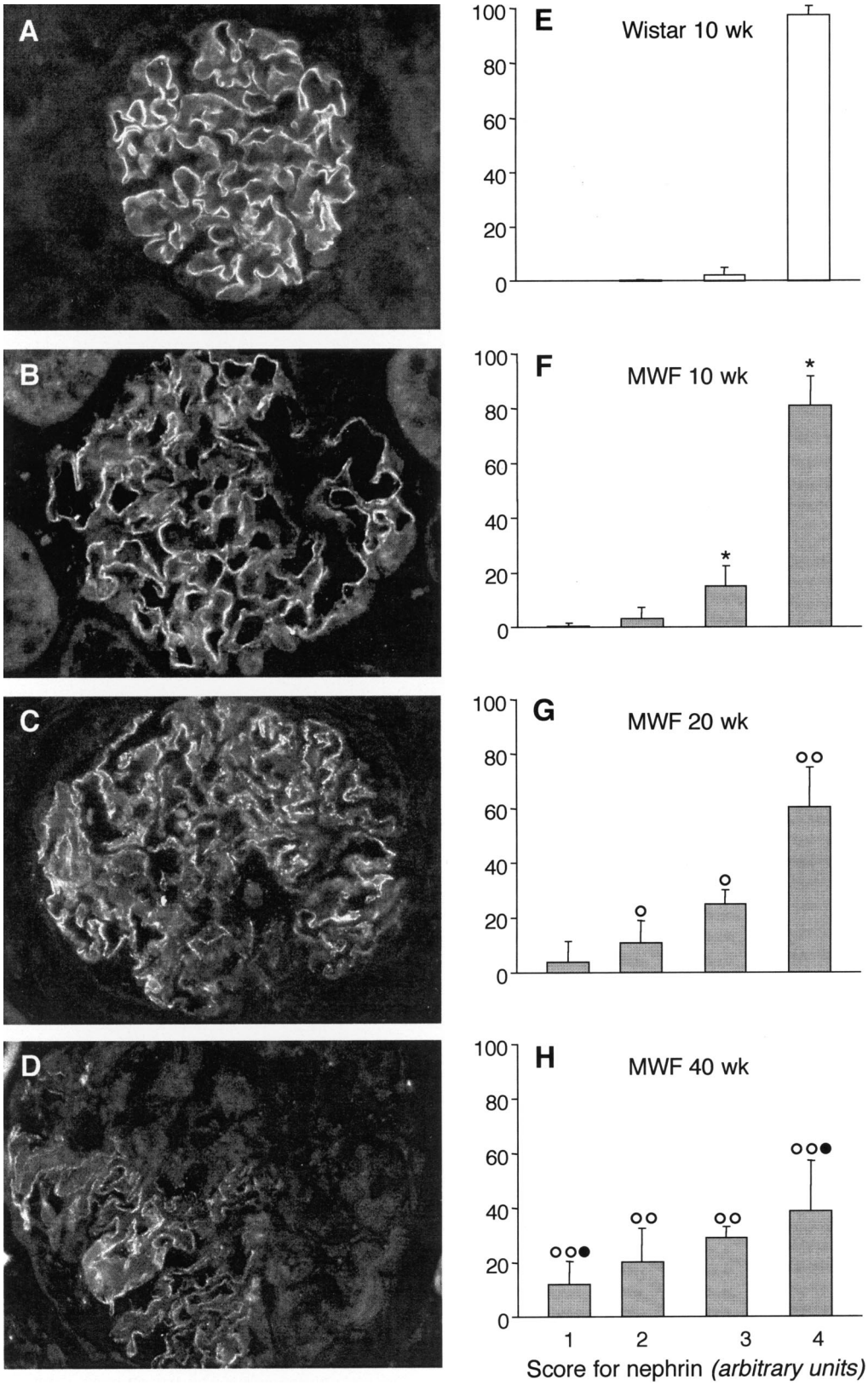

Figure 6. Glomerular nephrin expression. Representative images of immunostaining for nephrin in Wistar (**A**) and MWF rats (**B:** 10 weeks; **C:** 20 weeks; and **D:** 40 weeks). Final magnification, ×400. **E–H:** Semiquantitative analysis of nephrin expression in individual glomeruli (see Materials and Methods for details). Results are means ± SD ($n = 7$ rats for Wistar group and $n = 9$ to 10 rats for MWF groups). *$P < 0.01$ versus the 10-week-old Wistar rats; ○, $P < 0.05$ and ○○, $P < 0.01$ versus the 10-week-old MWF rats; ●, $P < 0.01$ versus the 20-week-old MWF rats.

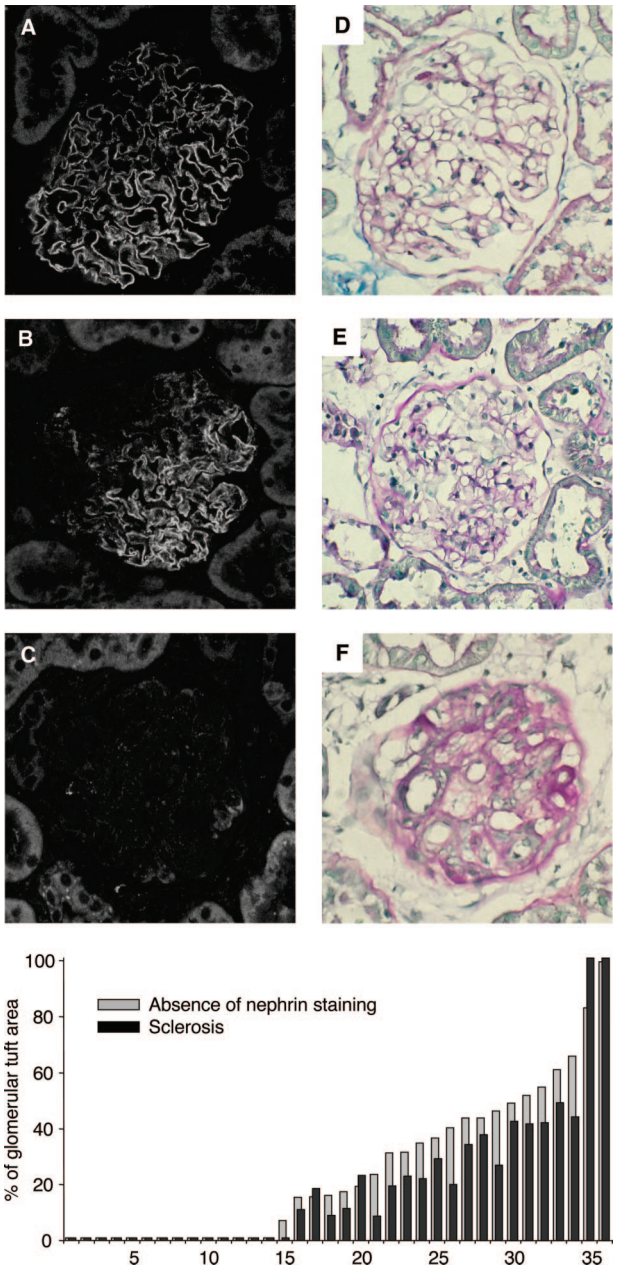

Figure 7. Immunofluorescent images of glomerular tuft immunostained for nephrin (**A–C**) and the corresponding glomerular sections stained with PAS at optical microscopy (**D–E**). The histogram shows the percentage of sclerosis (**black bars**) and the percentage of capillary tuft in which nephrin staining is absent (**gray bars**) measured by morphometrical analysis in 36 glomerular sections from MWF rats at 40 weeks.

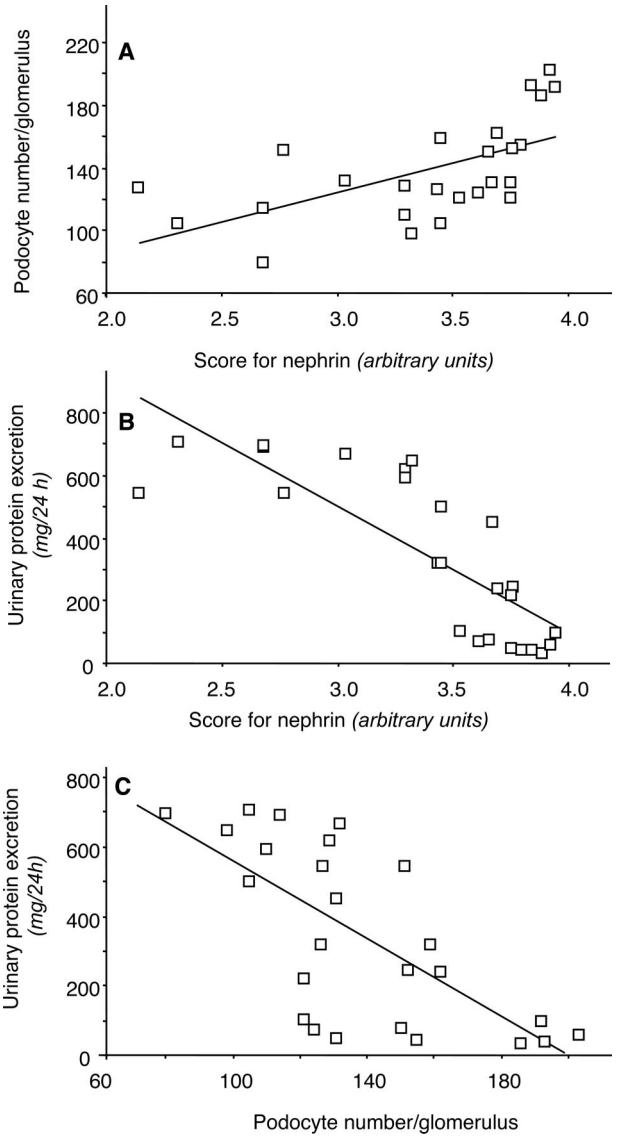

Figure 8. Plot of podocyte number per glomerulus (*y* axis) against the mean score for nephrin (*x* axis) (**A**) and of proteinuria (*y* axis) against the mean score for nephrin (*x* axis) (**B**) and the podocyte number per glomerulus (*x* axis) (**C**) in MWF rats. In each case, a significant correlation was found.

mals at 40 weeks of age. This suggests that early changes in nephrin staining in the MWF rats reflect protein redistribution, whereas later reduction of nephrin expression represents an actual decrease in the podocyte number and development of focal areas of sclerosis.

Compared with Wistar rats, MWF rats have a relative paucity of podocytes, and on glomerular volume expansion, these would be exposed to higher mechanical loading due to the greater surface area of glomerular capillary loops covered by each podocyte. It is known that mechanical stretch increases the synthesis of angiotensin II (AII) and angiotensin type 1 receptor in cultured podocytes and triggers apoptosis through AII-induced TGF-β production.[42] Even though glomerular capillary pressure is normal in the MWF strain,[43–45] podocyte stretching may occur as a dynamic adaptation to glomerular volume enlargement. Local activation of the angiotensin system in podocytes may also occur *in vivo*, initiating a vicious cycle that favors the progressive loss of podocytes responsible for the impairment of the glomerular barrier. This hypothesis is supported by the consistent observation that MWF rats are peculiarly sensitive to the renoprotective action of AII blockers.[46]

In conclusion, the present study shows that the massive proteinuria that develops spontaneously with age in male MWF rats is associated with glomerular hypertrophy and progressive reduction in podocyte number per glomerulus. Podocyte depletion positively correlates with

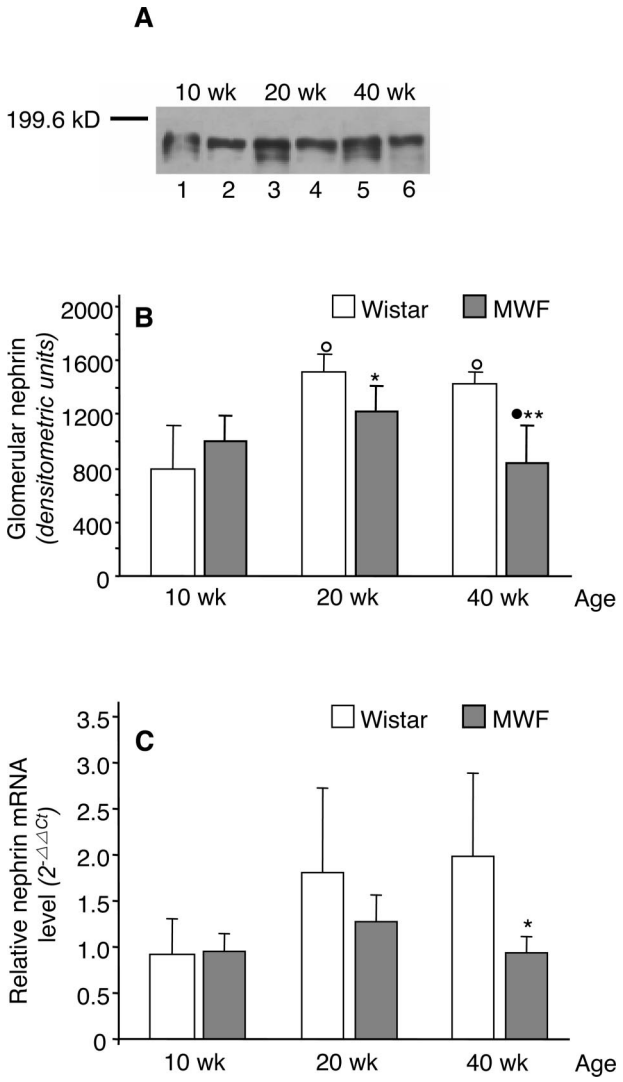

Figure 9. Protein and mRNA expression of nephrin. Western blot (**A**) and densitometric analysis (**B**) of nephrin in glomerular lysates from Wistar and MWF rats. Blots were probed with a rabbit anti-rat nephrin antibody raised against an intracellular site peptide of 21 amino acids (representative of four experiments). In Wistar rats, nephrin was detected as a doublet consisting of a major band of about 180 kd and a weak immunoband of lower molecular mass. **Lanes 1, 3,** and **5,** Wistar rats; **lanes 2, 4,** and **6,** MWF rats. Results are means ± SD ($n = 4$ rats for each Wistar group and $n = 4$ to 7 rats for MWF groups). *$P < 0.05$ and **$P < 0.01$ versus Wistar rats of the same age; ○, $P < 0.01$ versus the 10-week-old rats within the same strain; ●, $P < 0.05$ versus the 20-week-old rats within the same strain. **C:** Nephrin mRNA were quantified using real-time PCR in the cortical portion of the kidney from Wistar and MWF rats. Mean ΔCt of 10-week-old Wistar rats was taken as reference value to calculate $2^{-\Delta\Delta Ct}$ values for both strains. Results are means ± SD ($n = 5$ to 6 rats for each group). *$P < 0.05$ versus Wistar rats of the same age.

altered glomerular expression of the slit diaphragm-associated protein nephrin, suggesting that this event importantly contributes to podocyte dysfunction, subsequent impairment of the permselective properties of the glomerular filtration barrier and later progression to glomerulosclerosis.

Acknowledgment

We thank Mr. Piero Pellin for excellent technical assistance during SEM analysis.

References

1. Pavenstadt H, Kriz W, Kretzler M: Cell biology of the glomerular podocyte. Physiol Rev 2003, 83:253–307
2. Ly J, Alexander M, Quaggin SE: A podocentric view of nephrology. Curr Opin Nephrol Hypertens 2004, 13:299–305
3. Chugh SS, Kaw B, Kanwar YS: Molecular structure-function relationship in the slit diaphragm. Semin Nephrol 2003, 23:544–555
4. Tryggvason K, Pettersson E: Causes and consequences of proteinuria: the kidney filtration barrier and progressive renal failure. J Intern Med 2003, 254:216–224
5. Kerjaschki D: Caught flat-footed: podocyte damage and the molecular bases of focal glomerulosclerosis. J Clin Invest 2001, 108:1583–1587
6. Shirato I, Sakai T, Kimura K, Tomino Y, Kriz W: Cytoskeletal changes in podocytes associated with foot process effacement in Masugi nephritis. Am J Pathol 1996, 148:1283–1296
7. Whiteside CI, Cameron R, Munk S, Levy J: Podocytic cytoskeletal disaggregation and basement-membrane detachment in puromycin aminonucleoside nephrosis. Am J Pathol 1993, 142:1641–1653
8. Kurihara H, Anderson JM, Kerjaschki D, Farquhar MG: The altered glomerular filtration slits seen in puromycin aminonucleoside nephrosis and protamine sulfate-treated rats contain the tight junction protein ZO-1. Am J Pathol 1992, 141:805–816
9. Remuzzi A, Puntorieri S, Alfano M, Macconi D, Abbate M, Bertani T, Remuzzi G: Pathophysiologic implications of proteinuria in a rat model of progressive glomerular injury. Lab Invest 1992, 67:572–579
10. Macconi D, Ghilardi M, Bonassi ME, Mohamed EI, Abbate M, Colombi F, Remuzzi G, Remuzzi A: Effect of angiotensin-converting enzyme inhibition on glomerular basement membrane permeability and distribution of zonula occludens-1 in MWF rats. J Am Soc Nephrol 2000, 11:477–489
11. Seefeldt T, Bohman S-O, Gundersen HJG, Maunsbach AB, Pertersen VP, Olsen S: Quantitative relationship between glomerular foot process width and proteinuria in glomerulosclerosis. Lab Invest 1981, 44:541–546
12. Kawachi H, Kurihara H, Topham PS, Brown D, Shia MA, Orikasa M, Shimizu F, Salant DJ: Slit diaphragm-reactive nephritogenic MAb 5–1-6 alters expression of ZO-1 in rat podocytes. Am J Physiol 1997, 273:F984–F993
13. Liu G, Kaw B, Kurfis J, Rahmanuddin S, Kanwar YS, Chugh SS: Neph1 and nephrin interaction in the slit diaphragm is an important determinant of glomerular permeability. J Clin Invest 2003, 112:209–221
14. Kim YH, Goyal M, Kurnit D, Wharram B, Wiggins J, Holzman L, Kershaw D, Wiggins R: Podocyte depletion and glomerulosclerosis have a direct relationship in the PAN-treated rat. Kidney Int 2001, 60:957–968
15. Kuhlmann A, Haas CS, Gross ML, Reulbach U, Holzinger M, Schwarz U, Ritz E, Amann K: 1,25-Dihydroxyvitamin D3 decreases podocyte loss and podocyte hypertrophy in the subtotally nephrectomized rat. Am J Physiol Renal Physiol 2004, 286:F526–F533
16. Gross ML, El-Shakmak A, Szabo A, Koch A, Kuhlmann A, Munter K, Ritz E, Amann K: ACE-inhibitors but not endothelin receptor blockers prevent podocyte loss in early diabetic nephropathy. Diabetologia 2003, 46:856–868
17. Pagtalunan ME, Miller PL, Jumping-Eagle S, Nelson RG, Myers BD, Rennke HG, Coplon NS, Sun L, Meyer TW: Podocyte loss and progressive glomerular injury in type II diabetes. J Clin Invest 1997, 99:342–348
18. Meyer TW, Bennett PH, Nelson RG: Podocyte number predicts long-term urinary albumin excretion in Pima Indians with type II diabetes and microalbuminuria. Diabetologia 1999, 42:1341–1344
19. Steffes MW, Schmidt D, McCrery R, Basgen JM: Glomerular cell number in normal subjects and in type 1 diabetic patients. Kidney Int 2001, 59:2104–2113
20. White KE, Bilous RW, Marshall SM, El Nahas M, Remuzzi G, Piras G, De Cosmo S, Viberti G: Podocyte number in normotensive type 1 diabetic patients with albuminuria. Diabetes 2002, 51:3083–3089
21. White KE, Bilous RW: Structural alterations to the podocyte are related to proteinuria in type 2 diabetic patients. Nephrol Dial Transplant 2004, 19:1437–1440
22. Dalla Vestra M, Masiero A, Roiter AM, Saller A, Crepaldi G, Fioretto P:

Is podocyte injury relevant in diabetic nephropathy? Studies in patients with type 2 diabetes. Diabetes 2003, 52:1031–1035
23. Morigi M, Galbusera M, Binda E, Imberti B, Gastoldi S, Remuzzi A, Zoja C, Remuzzi G: Verotoxin-1-induced up-regulation of adhesive molecules renders microvascular endothelial cells thrombogenic at high shear stress. Blood 2001, 98:1828–1835
24. Topham PS, Kawachi H, Haydar SA, Chugh S, Addona TA, Charron KB, Holzman LB, Shia M, Shimizu F, Salant DJ: Nephritogenic mAb 5-1-6 is directed at the extracellular domain of rat nephrin. J Clin Invest 1999, 104:1559–1566
25. Mundlos S, Pelletier J, Darveau A, Bachmann M, Winterpacht A, Zabel B: Nuclear localization of the protein encoded by the Wilms' tumor gene WT1 in embryonic and adult tissues. Development 1993, 119:1329–1341
26. Weibel ER: Practical methods for biological morphometry. Stereological Methods. London, Academic Press, 1979, pp 40–116
27. Kawachi H, Koike H, Kurihara H, Yaoita E, Orikasa M, Shia MA, Sakai T, Yamamoto T, Salant DJ, Shimizu F: Cloning of rat nephrin: expression in developing glomeruli and in proteinuric states. Kidney Int 2000, 57:1949–1961
28. Fassi A, Sangalli F, Maffi R, Colombi F, Mohamed EI, Brenner BM, Remuzzi G, Remuzzi A: Progressive glomerular injury in the MWF rat is predicted by inborn nephron deficit. J Am Soc Nephrol 1998, 9:1399–1406
29. Olivetti G, Anversa P, Melissari M, Loud AV: Morphometry of the renal corpuscle during postnatal growth and compensatory hypertrophy. Kidney Int 1980, 17:438–454
30. Adamczak M, Gross ML, Krtil J, Koch A, Tyralla K, Amann K, Ritz E: Reversal of glomerulosclerosis after high-dose enalapril treatment in subtotally nephrectomized rats. J Am Soc Nephrol 2003, 14:2833–2842
31. Barisoni L, Kriz W, Mundel P, D'Agati V: The dysregulated podocyte phenotype: a novel concept in the pathogenesis of collapsing idiopathic focal segmental glomerulosclerosis and HIV-associated nephropathy. J Am Soc Nephrol 1999, 10:51–61
32. Floege J, Alpers CE, Sage EH, Pritzl P, Gordon K, Johnson RJ, Couser WG: Markers of complement-dependent and complement-independent glomerular visceral epithelial cell injury in vivo: expression of antiadhesive proteins and cytoskeletal changes. Lab Invest 1992, 67:486–497
33. Bacallao R, Fine LG: Molecular events in the organization of renal tubular epithelium: from nephrogenesis to regeneration. Am J Physiol 1989, 257:F913–F924
34. Schiffer M, Bitzer M, Roberts IS, Kopp JB, ten Dijke P, Mundel P, Bottinger EP: Apoptosis in podocytes induced by TGF-beta and Smad7. J Clin Invest 2001, 108:807–816
35. Pippin JW, Durvasula R, Petermann A, Hiromura K, Couser WG, Shankland SJ: DNA damage is a novel response to sublytic complement C5b-9-induced injury in podocytes. J Clin Invest 2003, 111:877–885
36. Kihara I, Tsuchida S, Yaoita E, Yamamoto T, Hara M, Yanagihara T, Takada T: Podocyte detachment and epithelial cell reaction in focal segmental glomerulosclerosis with cellular variants. Kidney Int Suppl 1997, 63:S171–S176
37. Petermann AT, Pippin J, Krofft R, Blonski M, Griffin S, Durvasula R, Shankland SJ: Viable podocytes detach in experimental diabetic nephropathy: potential mechanism underlying glomerulosclerosis. Nephron Exp Nephrol 2004, 98:e114–e123
38. Vogelmann SU, Nelson WJ, Myers BD, Lemley KV: Urinary excretion of viable podocytes in health and renal disease. Am J Physiol Renal Physiol 2003, 285:F40–F48
39. Nakamura T, Ushiyama C, Suzuki S, Hara M, Shimada N, Ebihara I, Koide H: Urinary excretion of podocytes in patients with diabetic nephropathy. Nephrol Dial Transplant 2000, 15:1379–1383
40. Drumond MC, Deen WM: Hindered transport of macromolecules through a single row of cylinders: application to glomerular filtration. J Biomech Eng 1995, 117:414–422
41. Daniels BS, Deen WM, Mayer G, Meyer T, Hostetter TH: Glomerular permeability barrier in the rat: functional assessment by in vitro methods. J Clin Invest 1993, 92:929–936
42. Durvasula RV, Petermann AT, Hiromura K, Blonski M, Pippin J, Mundel P, Pichler R, Griffin S, Couser WG, Shankland SJ: Activation of a local tissue angiotensin system in podocytes by mechanical strain. Kidney Int 2004, 65:30–39
43. Remuzzi A, Puntorieri S, Mazzoleni A, Remuzzi G: Sex related differences in glomerular ultrafiltration and proteinuria in Munich-Wistar rats. Kidney Int 1988, 34:481–486
44. Remuzzi A, Puntorieri S, Battaglia C, Bertani T, Remuzzi G: Angiotensin converting enzyme inhibition ameliorates glomerular filtration of macromolecules and water and lessens glomerular injury in the rat. J Clin Invest 1990, 85:541–549
45. Remuzzi A, Imberti O, Puntorieri S, Malanchini B, Macconi D, Magrini L, Bertani T, Remuzzi G: Dissociation between antiproteinuric and antihypertensive effect of angiotensin converting enzyme inhibitors in rats. Am J Physiol 1994, 267:F1034–F1044
46. Remuzzi A, Benigni A, Malanchini B, Bruzzi I, Foglieni C, Remuzzi G: ACE inhibition prevents renal failure and death in uninephrectomized MWF/Ztm rats. Kidney Int 1995, 47:1319–1326